NANO LETTERS

2007
Vol. 7, No. 4
1022−1025

Power Generation by Pressure-Driven Transport of Ions in Nanofluidic Channels

Frank H. J. van der Heyden, Douwe Jan Bonthuis, Derek Stein, Christine Meyer, and Cees Dekker*

Kavli Institute of Nanoscience, Delft University of Technology, Lorentzweg 1, 2628 CJ Delft, The Netherlands

Received January 24, 2007; Revised Manuscript Received February 9, 2007

ABSTRACT

We report on the efficiency of electrical power generation in individual rectangular nanochannels by means of streaming currents, the pressure-driven transport of counterions in the electrical double layer. Our experimental study as a function of channel height and salt concentration reveals that the highest efficiency occurs when double layers overlap, which corresponds to nanoscale fluidic channels filled with aqueous solutions of low ionic strength. The highest efficiency of ~3% was found for a 75 nm high channel, the smallest channel measured. The data are well described by Poisson–Boltzmann theory with an additional electrical conductance of the Stern layer.

A pressure-driven flow through a fluidic channel induces a flow of counter charges in the double layer at the channel walls, thus generating an electrical current (Figure 1a). When this so-called streaming current is driven through an external load resistor R_L, electrical energy is harvested from the fluidic system. The notion of generating electrical power in this way is not new,[1] yet has received renewed attention in the context of micro- and nanofluidic devices,[2−7] whose geometries and material properties can be engineered. Moreover, nanoscale fluidic devices allow the probing of the regime of double-layer overlap, where the energy conversion efficiency is expected to be highest.[5−7]

The power output and energy conversion efficiency, ε, have been modeled for fluidic devices with various geometries by calculating their electrokinetic response properties using the Navier−Stokes description of the fluid flow and the Poisson−Boltzmann (PB) description of the electrostatic ion distributions in the diffuse layer.[1−6,8] Using approximations of the PB solution and a constant surface potential ζ as the electrical boundary condition,[1−4] ε was predicted to increase as function of salt concentration n.[3] In contrast, we recently calculated that ε decreases as function of n based on an exact solution of PB with a constant surface charge σ as a more appropriate boundary condition for silica.[6] Our model also predicts that: (i) ε is independent of n in the regime of strong double-layer overlap, i.e., for low n in nanoscale channels, (ii) ε decreases as function of the counterion mobility, and (iii) ε does not depend strongly on the channel height as long as double layers overlap.[9]

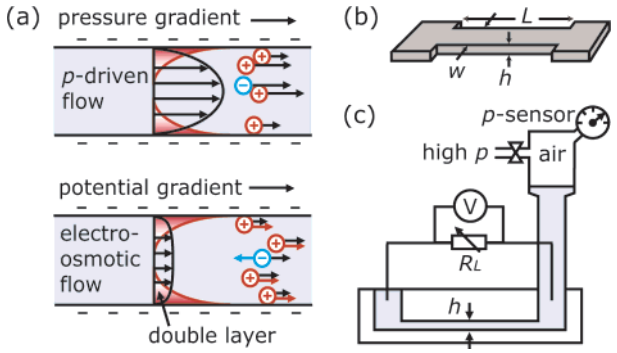

Figure 1. (a) Schematic illustration of electrokinetic effects. Top: A pressure-driven flow carries the net ionic charge within the double layer, generating a streaming current. Bottom: A potential gradient generates both an electro-osmotic fluid flow (black arrows) and an additional electrophoretic ion velocity (colored arrows). (b) Three-dimensional channel geometry. (c) Side view of the nanochannel, including the pressure and electrical connections.

Experimental studies of electrokinetic power generation have focused on porous glass because its many parallel channels make this material a good candidate for obtaining appreciable powers.[4,5] However, the poor control over the geometry and surface properties in porous silica complicates quantitative testing of the physical models.

In this letter, we present an experimental study of electrokinetic power generation in individual rectangular nanofluidic channels whose geometries remain well-defined down to the regime where double layers overlap. Our measurements of the generated streaming potential ΔV across the nanochannel as a function of applied pressure Δp and

* Corresponding author. E-mail: dekker@mb.tn.tudelft.nl.

10.1021/nl070194h CCC: $37.00
Published on Web 03/13/2007

R_L are excellently described by a linear electrokinetic response model. The highest power (up to 240 pW for a single 490 nm high channel) and efficiency (up to 3.2% for a 75 nm high channel) are found for low n. The energy conversion efficiency of our silica channels is limited by a Stern layer conductance of 10−30 pS, which provides an additional pathway for power dissipation.

Nanochannels of width $w = 50\ \mu$m, length $L = 4.5$ mm, and height h (Figure 1b) were fabricated between 1.5 × 1.5 mm^2 reservoirs in fused silica using a direct bonding method.[10] Details of the experimental setup and the streaming current measurement procedure are described elsewhere.[11] Potassium chloride (KCl) and lithium chloride (LiCl) solutions were prepared by the serial dilution of a 1 M stock solution with 10 mM HEPES buffer (pH = 7.5) in distilled, deionized water (18 MΩcm). A load resistor R_L, adjustable between 0.1 and 100 GΩ in steps of 0.1 GΩ, was connected between the Ag/AgCl electrodes at each channel end (Figure 1c). The potential difference ΔV across R_L was measured for each applied pressure difference Δp.

The voltage difference ΔV, generated when a pressure-driven streaming current flows through an external load resistor, is observed to increase linearly with Δp for various KCl concentrations, [KCl] (Figure 2a). For a constant Δp, ΔV is found to increase with R_L (Figure 2b) until reaching a saturation value at high R_L. ΔV was higher for lower [KCl] across the full range of load resistances. Figure 2c reveals that the generated power $P = \Delta V^2/R_L$, calculated from the data in Figure 2b, peaks at a particular value of R_L. The highest power from a single 490 nm high silica nanochannel was ∼240 pW, obtained for $R_L = 55$ GΩ and [KCl] = 10^{-5} M. ΔV and P did not change with n for [KCl] ≲ $10^{-4.5}$ M.[12]

We model the energy conversion ability of our fluidic channel by the electrical equivalent circuit of Figure 2d.[6] The channel device is characterized through its electrokinetic response properties, which relate the liquid volume flow Q and the electrical current I to the applied driving forces Δp and ΔV. We define the streaming conductance $S_{str} \equiv dI/d\Delta p$,[11] the electrical resistance $R_{ch} \equiv d\Delta V/dI$, and the fluidic impedance $Z_{ch} \equiv d\Delta p/dQ = 12\eta L/wh^3$ for a slit-like channel containing a fluid of viscosity η. The potential difference for a given Δp is calculated to be $\Delta V = -(R_{ch}R_L/(R_{ch} + R_L))S_{str}\Delta p$. We observe from Figure 2a that ΔV scales linearly with Δp for constant R_L. The expression for ΔV is fitted to the measurements as function of R_L with constant Δp (Figure 2b), yielding S_{str} and R_{ch} as fit parameters at each salt concentration. The excellent quality of the fits confirms that the nanochannel is accurately characterized by its linear electrokinetic responses. Independent measurements of R_{ch}, measured by a V−I sweep, and S_{str} just before and after the power measurement corresponded to the fit values within a few percent. The equivalent circuit model predicts maxima in the power and efficiency as function of R_L, given by $P_{max} = (R_{ch}/4)S_{str}^2\Delta p^2$ at $R_L = R_{ch}$, and $\varepsilon_{max} = \alpha/(2 - \alpha + 2\sqrt{1-\alpha})$ at $R_L = R_{ch}/\sqrt{1-\alpha}$ with $\alpha = S_{str}^2 Z_{ch} R_{ch}$, respectively.[6]

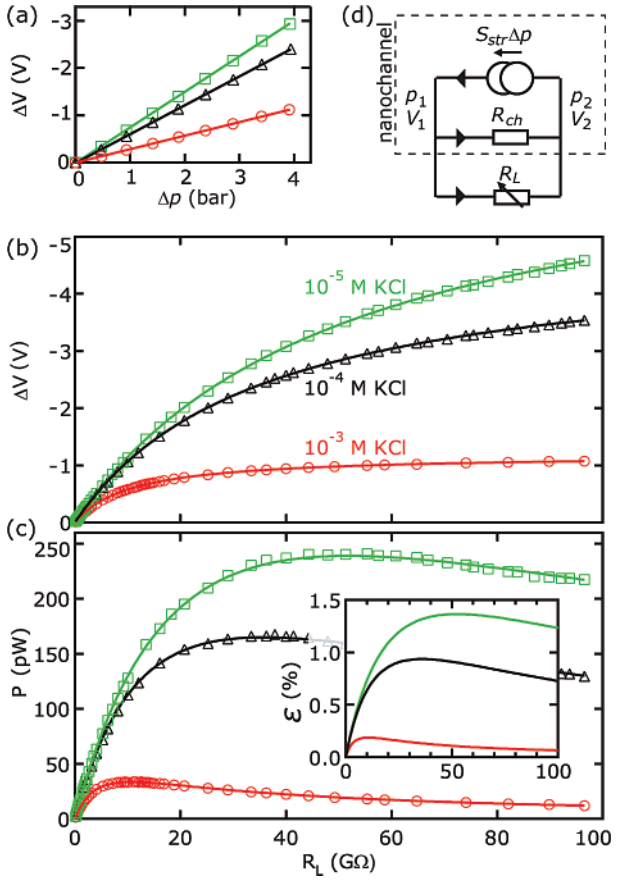

Figure 2. Measurements for various KCl concentrations in a 490 nm high silica nanochannel of (a) ΔV as function of Δp for R_L = 50 GΩ, and (b) ΔV and (c) $P = \Delta V^2/R_L$ as function of R_L for Δp = 4 bar. Lines are fits to the equivalent electronic circuit model of the nanochannel connected to R_L, as depicted in (d). The fit parameters S_{str} and R_{ch} are used to calculate the efficiency (inset). We define $\Delta p = p_2 - p_1$ and $\Delta V = V_2 - V_1$. The arrows indicate the ionic current directions for a positive applied Δp during power generation.

The saturation behavior of ΔV as function of R_L, and the resulting maxima in P and ε, can be understood intuitively by considering the model circuit of Figure 2d: For small load resistors ($R_L \ll R_{ch}$), the streaming current, $S_{str}\Delta p$, will mainly flow through R_L, generating a small potential difference proportional to R_L, $\Delta V \simeq -S_{str}\Delta p R_L$, whereas for very large load resistances ($R_L \gg R_{ch}$), most current will flow back through the channel itself, generating the saturation potential $\Delta V \approx -S_{str}\Delta p R_{ch}$. The increase of P for small R_L, the decrease for high R_L, and the maximum in between then follow directly from $P = \Delta V^2/R_L$. Because the energy conversion efficiency is defined as the output power P divided by the input power, which is mainly consumed by viscous dissipation, ε and P show nearly identical behavior as function of R_L (Figure 2c).

Figure 3 shows our experimental study of ε as function of salt concentration, channel height, and counterion type in individual rectangular nanofluidic channels. It reveals that the highest efficiency occurs in the regime of double-layer overlap. S_{str} and R_{ch} (Figure 3a and b) are obtained through fits of ΔV versus R_L for each measured salt concentration, from which P_{max} and ε_{max} are calculated (Figure 3c and d).

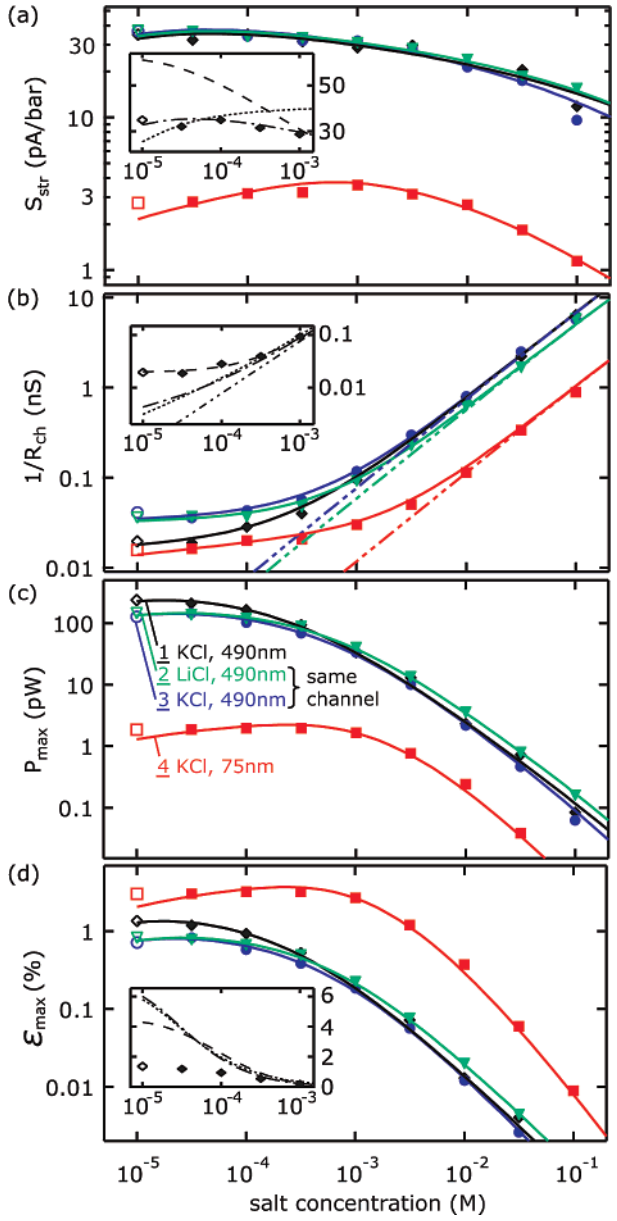

Figure 3. Experimental results for S_{str}, $1/R_{ch}$, P_{max}, and ε_{max} as function of salt concentration with $\Delta p = 4$ bar. Numbered colors indicate different measurements, with the channel height and ion type indicated in (c). 1 and 4 are our experiments with the highest power and efficiency, respectively. 2 and 3 are typical for changing the counterion type in the same channel. Open symbols indicate that for $n = 10^{-5}$ the bulk conductivity was enhanced by protons.[12] Lines represent different electrical boundary conditions for the silica surface: a constant $\sigma = -8.2$ mC/m^2 (dashed lines; insets), a constant $\zeta = -100$ mV (dotted lines; insets), and a chemically varying σ with either $G_{Stern} = 0$ (dash−dotted lines; insets) or $G_{Stern} \neq 0$ (solid lines; main panels). The dash−dot−dotted curves in (b) indicate the bulk conductance. The parameter values for the chemically varying σ model[14] with fixed $\Gamma = 8$ nm^{-2} and pH = 7.5 were found to be p$K = 8.4$, 8.3, 8.2, 7.5 and $C = 2.9$, 2.5, 0.8, 0.15 Fm^{-2}, and G_{Stern} was 14, 30, 30, 8.5 pS for 1, 2, 3, 4, respectively. These values are similar to values found earlier for silica.[11,15] All curves were calculated using the liquid and salt properties in ref 16.

The streaming conductance was approximately constant with salt concentration at low n and then dropped at higher n. The channel conductance on the other hand was constant at low n and increased at higher n.[12] P_{max} and ε_{max} were about constant at low n and decreased strongly at higher n. The transition between these salt regimes occurred at higher salt concentrations for smaller channels, viz., at $10^{-3.5}$ M for $h = 75$ nm versus $10^{-4.5}$ M for $h = 490$ nm. In the regime of maximum efficiency and power (low n), we found that R_{ch} and ε_{max} were 2−3 times larger for the small channels, whereas S_{str} and P were respectively 1 and 2 orders of magnitude larger for the big channels (Table 1). Changing the counterion type in the same channel barely affected the conductance for low n.[13] For high n, KCl resulted in a ∼30% higher conductance than LiCl, which is consistent with the difference in bulk conductivity.

Table 1. Channel Height Dependence of S_{str}, $1/R_{ch}$, P_{max}, and ε_{max} (Mean ± Standard Deviation) for the Regime of Maximum Effciency (Low n)[a]

h (nm)	S_{str} (pA/bar)[17]	$1/R_{ch}$ (nS)	P_{max} (pW)	ε_{max} (%)
75	2.2 ± 0.3	11 ± 2	1.7 ± 0.3	2.8 ± 0.5
490	34 ± 3	26 ± 7	190 ± 60	1.1 ± 0.4

[a] In this regime, the Stern conductance dominates the channel conductance ($G_{Stern} \approx 1/R_{ch}$). Eight channels of $h = 75$ nm, and thirteen channels of $h = 490$ nm were measured.

Predictions of the salt dependence of S_{str} and R_{ch}, based on the exact PB solution for the diffuse layer in a slitlike geometry, are strongly affected by the electrical properties of the channel walls (insets Figure 3). A constant ζ fails to describe the salt dependence of either S_{str} or R_{ch} (dotted lines). A constant $\sigma = -8.2$ mC/m^2 describes R_{ch} accurately but overestimates S_{str} (dashed curves), whereas a chemically varying σ, where σ increases as function of n due to the chemical equilibrium of the charge determining silanol groups at the silica surface,[14] describes S_{str} well but underestimates $1/R_{ch}$ (dash−dotted curves). All of the above boundary conditions result in an overestimate of ε_{max} (inset Figure 3d). No single boundary condition for the diffuse layer simultaneously describes the salt dependence of both S_{str} and R_{ch} accurately.

Our measurements can be well explained, however, if we consider the presence of a finite Stern layer conductance, G_{Stern}, at the surface. Mobile ions that are confined to the Stern layer (the first molecular layers adjacent to a charged surface) will contribute to the channel conductance without affecting the streaming conductance because Stern layer ions are presumed to move below the no-slip plane.[18−20] G_{Stern} depends on the mobility and density of ions in the Stern layer, for which several microscopic models exist with significantly varying predictions.[21] Surface properties such as the roughness, charge density, and chemical composition are also known to affect G_{Stern}.[22] Our simultaneous measurements of S_{str} and R_{ch} in silica nanochannels, as well as our results for P_{max} and ε_{max}, are well described by a chemically varying σ for the diffuse layer with the addition of a constant G_{Stern} (thick solid lines in Figure 3). For our channels, we find values for G_{Stern} in the range of 10−30 pS.

The fact that we find the highest efficiency in the smallest $h = 75$ nm channels is largely caused by the lower Stern conductance found for these channels (Table 1) because the

Stern conductance provides an additional pathway for power dissipation that reduces the efficiency. In the absence of Stern conductance, the predicted maximum efficiency does not depend strongly on h as long as double layers overlap.[6] The finite Stern conductance at the silica surface also cancels the predicted ion mobility dependence of ε_{max} at low salt, where G_{Stern} dominates the channel conductance. The reason why G_{Stern} is lower for smaller channels could be rooted in the fabrication process, as the shorter etching may result in a lower surface roughness,[23] or it may be due to charge regulation effects, which become increasingly important for decreasing h. Reducing the channel height below 75 nm may therefore improve the efficiency through a further reduction in Stern conductance, but not because of any effect predicted for ideal channels. A systematic investigation of the microscopic origins of the Stern conductance should provide insight into how it can be minimized and whether decreasing the channel height is a critical parameter to achieve this. Our electrokinetic method provides a sensitive tool to conduct such studies.

Our observation that the Stern conductance barely changed when Li^+ replaced K^+ in the same channel for low n is quite remarkable[13] because their bulk mobilities differ by a factor of 2. The similarity of G_{Stern} for K^+ and Li^+ counterions suggests that protons dominate the Stern conductance. Conduction by protons can be very efficient through the mechanism of hopping between water molecules.[24] Indeed, it has already been suggested that protons are mobile and K^+ and Li^+ immobile in the Stern layer at the silica surface.[20]

In conclusion, we have obtained first measurements of electrokinetic power generation in individual nanofluidic channels. The data are excellently described by characterizing the fluidic device through its linear electrokinetic response properties. Our analysis of the efficiency reveals two distinct salt concentration regimes: the efficiency is highest at low salt when double layers overlap in our nanoscale channels, and drops at higher salt. This is well described by modeling the boundary of the diffuse layer by a chemically varying surface charge and invoking a Stern layer conductance. The Stern conductance was found to be almost the same for counterions with very different bulk mobilities, suggesting that protons dominate the Stern conductance on silica. The highest efficiency of 3.2% was found for the smallest 75 nm high channel. Reducing the Stern conductance would substantially improve the efficiency and should be the prime focus of future experimental work.

Acknowledgment. We acknowledge funding from NWO, FOM, and NanoNed.

References

(1) Osterle, J. F. *J. Appl. Mech.* **1964**, *31*, 161.
(2) Chun, M.-S.; Lee, T. S.; Choi, N. W. *J. Micromech. Eng.* **2005**, *15*, 710.
(3) Yang, J.; Lu, F.; Kostiuk, L. W.; Kwok, D. Y. *J. Micromech. Microeng.* **2003**, *13*, 963.
(4) Olthuis, W.; Schippers, B.; Eijkel, J.; van den Berg, A. *Sens. Actuators, B* **2005**, *111*, 385.
(5) Lu, M.-C.; Satyanarayana, S.; Karnik, R.; Majumdar, A.; Wang, C.-C. *J. Micromech. Microeng.* **2006**, *16*, 667.
(6) van der Heyden, F. H. J.; Bonthuis, D. J.; Stein, D.; Meyer, C.; Dekker, C. *Nano Lett.* **2006**, *6*, 2232.
(7) Daiguji, H.; Yang, P.; Szeri, A. J.; Majumdar, A. *Nano Lett.* **2004**, *4*, 2315. Daiguji, H.; Oka, Y.; Adachi, T.; Shirono, K. *Electrochem. Commun.* **2006**, *8*, 1796.
(8) The Poisson−Nernst−Planck equations govern the distribution of ions in a fluidic channel, which reduce to the PB equation for a system in thermodynamic equilibrium. Typical nonequilibrium effects, which are generally nonlinear, can occur at the channel entrance.[7] Nonlinear entrance effects were not observed in our nanochannels, which are very long. We thus may use PB theory, which provides convenient analytical expressions and linear electrokinetic responses.[6]
(9) These predictions hold for an optimized R_L. The h and mobility dependence assume strong double-layer overlap, and a value for σ in the range $0.2 \lesssim h\sigma \lesssim 2$ nm × C/m^2.
(10) van der Heyden, F. H. J.; Stein, D.; Besteman, K.; Lemay, S. G.; Dekker, C. *Phys. Rev. Lett.* **2006**, *96*, 224502.
(11) van der Heyden, F. H. J.; Stein, D.; Dekker, C. *Phys. Rev. Lett.* **2005**, *95*, 116104.
(12) For measurements at low salt, $n \leq 10^{-4}$ M, S_{str} and R_{ch} exhibited a slow drift of typically a few percent per hour, resulting in scatter in the data. This drift can be attributed to a changing σ due to aging[25] or a drifting pH. The independently measured bulk conductivity of the solution corresponded to tabulated values[26] down to $n \leq 10^{-4.5}$ M. For lower n, protons from dissociated water molecules in equilibrium with dissolved CO_2 enhance the conductivity, corresponding to a pH of about 5.5 for our solutions. In nanochannels, $1/R_{ch}$ already begins to deviate from the bulk values at $n \leq 10^{-3}$ M (Figure 3b) due to the dominance of counterions in the double layer.
(13) We found in three separate measurements that $1/R_{ch}$ was only 13 ± 17% higher for $10^{-4.5}$ KCl relative to $10^{-4.5}$ LiCl, while the mobility of K^+ ions is about 90% higher compared to Li^+ ions. For $n = 10^{-4.5}$, $G_{Stern} \approx 1/R_{ch}$ and the conductivity in the diffuse layer is still dominated by the salt counterions,[12] even if we account for the slightly enhanced proton concentration due to diffusion towards the channel entrance.[7]
(14) Behrens, S. H.; Grier, D. G. *J. Chem. Phys.* **2001**, *115*, 6716.
(15) Löbbus et al. (Löbbus, M.; Sonnfeld, J.; van Leeuwen, H. P.; Vogelsberger, W.; Lyklema, J. *J. Colloid Interface Sci.* **2000**, *229*, 174) found a Stern conductivity of $K^{\sigma i} = 1$ nS for the silica−water interface at pH = 7.4 and $[K^+] = 1$ mM, which translates to $G_{Stern} = 2wK^{\sigma i}/L = 22$ pS for our channel geometry.
(16) We used temperature $T = 296.15$ K; dielectrical constant $\epsilon = 79$; salt-corrected viscosities $\eta_{KCl} = \eta_{water}(1 - 0.01\ n)$ and $\eta_{LiCl} = \eta_{water}(1 + 0.148\ n)$, with $\eta_{water} = 0.93$ mPas; ion mobility $\mu = \lambda^0\gamma/F$, with Faraday constant F, limiting equivalent conductivities $\lambda^0 = 7.06$ (K^+), 3.72 (Li^+), and 7.33 (Cl^-) × 10^{-3} Sm^2 mol^{-1} (Coury, L. *Curr. Sep.* **1999**, *18*, 3) and salt correction factors $\gamma_{KCl} = 0.727 + 0.031\ e^{-n/0.0012} + 0.082\ e^{-n/0.033} + 0.16\ e^{-n/0.47}$ and $\gamma_{LiCl} = 0.585 + 0.035\ e^{-n/0.0013} + 0.090\ e^{-n/0.034} + 0.29\ e^{-n/0.54}$, found by fitting tabulated values.[26]
(17) Upon initially filling the $h = 75$ nm channels, S_{str} was often very low (<0.5 pA/bar) for hours. Over time, S_{str} creeped to stable values of ∼2 pA/bar.
(18) Lyklema, J. *J. Phys.: Condens. Matter* **2001**, *13*, 5027.
(19) Hunter, R. J. *Adv. Colloid Interface Sci.* **2003**, *100*, 153.
(20) Rosen, L. A.; Baygents, J. C.; Saville, D. A. *J. Chem. Phys.* **1993**, *98*, 4183.
(21) Proposed mobilities for ions in the Stern layer range from near-bulk values[18] to very low mobilities[20] to models that distinguished different populations with different mobilities within each ion type (Netz, R. R. *Phys. Rev. Lett.* **2003**, *91*, 138101).
(22) Zembala, M. *Adv. Colloid Interface Sci.* **2004**, *112*, 59.
(23) A rough surface can increase the thickness of the stagnant layer and the number of surface charges exposed to the liquid.[22]
(24) Anderson, J. H.; Parks, G. A. *J. Phys. Chem.* **1968**, *72*, 3662.
(25) Vigil, G.; Xu, Z.; Steinberg, S.; Israelachvili, J. *J. Colloid Interface Sci.* **1994**, *165*, 367.
(26) Weast, R., Ed. *CRC Handbook of Chemistry and Physics*, 61st ed.; CRC Press: Boca Raton, FL, 1980.

NL070194H